

The Ogden Model for Coronary Artery Mechanical Behaviors

Hui-Lung Chien¹, Bo Wun Huang², Jao-Hwa Kuang^{1*}

¹ Department of Mechanical and Electro-mechanical Engineering, National Sun Yat-sen University, Kaohsiung 80424, Taiwan, R.O.C.

² Graduate Institute of Mechatronics Engineering, Cheng Shiu University, Kaohsiung 83347, Taiwan, R.O.C.
kuang@faculty.nsysu.edu.tw

Abstract: A nonlinear coronary artery Ogden model is proposed to describe the possible artery mechanical behavior during the stent expansion process. The artery model parameters were curve fitted from measured coronary artery circumferential stress-stretch curves. The proposed Ogden model parameters were compared with the data cited from other literature. The proposed Ogden artery model employed to simulate stent inflation and deflation during its expansion process. The numerical results reveal that the proposed nonlinear Ogden model feasibly simulates the stent expansion process.

[Hui-Lung Chien, Bo Wun Huang, Jao-Hwa Kuang. **The Ogden Model for Coronary Artery Mechanical Behaviors**. Life Science Journal. 2011; 8(4):430-437] (ISSN:1097-8135). <http://www.lifesciencesite.com>.

Keywords: Ogden model; mechanical behavior; coronary artery; stent expansion.

1. Introduction

Stent implantation has been applied to treat arterial stenosis in last few decades. The finite element method has been frequently used to investigate stretch behaviors of artery, plaque and metal stent during implantation. Proper artery and plaque mechanical models play an important role in the simulation. In many pioneering works, different stress-stretch relationships have been proposed to describe artery mechanical behavior. These proposed artery models have been extensively studied for many years with much data investigated for various biomedical applications. The inflation-extension tests were used to measure the mechanical properties of disease-free and diseased coronary arteries for surgical development^[1-3]. The coronary artery stress-strain relationships yielded by inflation-extension tests were employed to compute the Green strain tensor components to establish a mathematical description of arterial behavior and determine the constitutive equation parameters for the different arterial wall layers^[4-6]. Tensile tests were utilized to investigate the stress-stretch curves of different human iliac artery layers and plaque to establish a constitutive atherosclerotic artery model^[7]. The mechanical properties of blood vessels of various sizes obtained using the tensile test were investigated. These blood vessels include human cerebral arteries and veins, and porcine abdominal aorta, vena cava, carotid arteries and iliac arteries^[8-11]. The uniaxial and biaxial tension tests were used to measure arterial elastin mechanical properties for determining the strain energy function and to investigate the elastic behavior of porcine coronary artery tissue for stent design studies and stent implantation simulations^[12-15].

The stent implantation has been applied to various arteries including intracranial arteries, coronary arteries, carotid arteries, iliac arteries and renal arteries^[16-19]. The stent-graft insertion has been used to open abdominal aorta aneurysms, thoracic aorta aneurysms and aortic arch aneurysms^[20-22]. Identifying the mechanical properties of arteries is necessary for stent implantation simulation research. Accordingly, the tensile stress-stretch curves of porcine coronary arteries were used to derive the artery model in this study. The nonlinear elastic Ogden strain energy function was employed to fit the measured data and applied to the finite element simulation of stent expansion in a coronary artery.

2. The Nonlinear Ogden Model of Coronary Artery

Based on the nonlinear solid mechanics, the principal stresses in an isotropic hyper-elastic material depend only upon principal stretches and can be expressed using the following relation^[23],

$$\sigma_i = J^{-1} \lambda_i \left(\frac{\partial \Psi}{\partial \lambda_i} \right) \quad \text{for } i = 1, 2, 3 \quad (1)$$

where σ_i : is the principal stress.

λ_i : is the principal stretch.

Ψ : is the strain energy function.

J : is the product of λ_1 , λ_2 , and λ_3 .

The strain energy function Ψ is a scalar-valued isotropic tensor function and can be expressed as follows,

$$\Psi = \Psi(\mathbf{C}) = \Psi(\mathbf{B}) \quad (2)$$

where \mathbf{C} : is the right Cauchy-Green tensor.

\mathbf{B} : is the left Cauchy-Green tensor.

The right and left Cauchy-Green tensors can be

expressed using the deformation gradient \mathbf{F} as the following equations, respectively.

$$\mathbf{C} = \mathbf{F}^T \mathbf{F}, \quad \text{and} \quad \mathbf{B} = \mathbf{F} \mathbf{F}^T \quad (3)$$

Because the biological soft tissue is an isotropic hyper-elastic material, the strain energy function may be expressed in terms of the independent strain invariants of symmetric Cauchy-Green tensors \mathbf{C} and \mathbf{B} as the following function

$$\begin{aligned} \Psi &= \Psi [I_1(\mathbf{C}), I_2(\mathbf{C}), I_3(\mathbf{C})] \\ &= \Psi [I_1(\mathbf{B}), I_2(\mathbf{B}), I_3(\mathbf{B})], \end{aligned} \quad (4)$$

Where the invariants I_i ($i=1, 2, 3$) can be expressed in terms of stretches as

$$I_1 = \lambda_1 + \lambda_2 + \lambda_3 \quad (5a)$$

$$I_2 = \lambda_1 \lambda_2 + \lambda_1 \lambda_3 + \lambda_2 \lambda_3 \quad (5b)$$

$$I_3 = \lambda_1 \lambda_2 \lambda_3 \quad (5c)$$

Therefore, the strain energy function can be expressed in terms of stretches as

$$\Psi = \Psi (\lambda_1, \lambda_2, \lambda_3) \quad (6)$$

A biological material can be regarded as

incompressible with the constraint condition $I_3 = J = \lambda_1 \lambda_2 \lambda_3 = 1$. Based on the relation between the strain energy function and the stretches and the constraint condition of incompressibility, Ogden proposed the strain energy function as^[23]

$$U = \sum_{n=1}^N \frac{\mu_n}{\alpha_n} (\lambda_1^{\alpha_n} + \lambda_2^{\alpha_n} + \lambda_3^{\alpha_n} - 3) \quad (7)$$

U denotes the strain energy function of the nonlinear elastic Ogden model. N is the item number. $\lambda_1, \lambda_2,$ and λ_3 are principal stretches. μ_n and α_n are material constants used in the Ogden model.

The nonlinear elastic coronary artery Ogden model is curve fitted from the measured stress-stretch relationships of arteries in this study. To illustrate the feasibility of the proposed models, these curve fitted models were employed in the finite element analysis to simulate the inflation and deflation of a coronary stent during its expansion process.

Table 1. Measured data for different specimens in the CS test

| specimen No. | measured dimensions | | | calculated values | loading rate (mm/min.) | strain rate (1/sec.) |
|--------------|-----------------------|----------------------|--|--------------------------------------|------------------------|----------------------|
| | length (L_0) (mm) | width (W_0) (mm) | arterial wall thickness (t_0) (mm) | specimen volume (V_0) (mm^3) | | |
| C1 | 13.3 | 4.39 | 0.725 | 79 | 4 | 0.023 % |
| C2 | 14.4 | 5.49 | 0.560 | 85 | | 0.019 % |
| C3 | 14.0 | 5.73 | 0.570 | 88 | | 0.019 % |
| C4 | 10.7 | 4.99 | 0.905 | 89 | | 0.017 % |
| C5 | 12.4 | 5.71 | 0.900 | 119 | | 0.016 % |
| C6 | 16.2 | 7.11 | 1.105 | 238 | | 0.013 % |
| C7 | 15.9 | 7.40 | 0.780 | 175 | | 0.015 % |

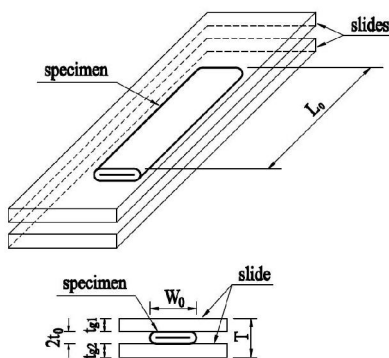


Figure 1. Dimension measurement for specimens used in the CS test

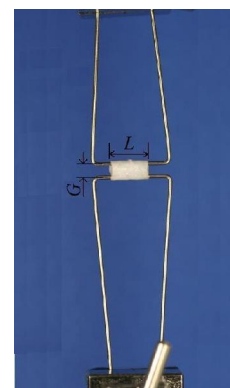


Figure 2. Measurement set up for the specimens in the CS test

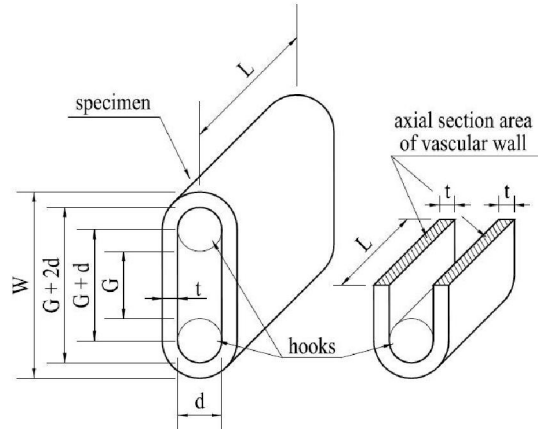


Figure 3. Sketch of artery specimen dimensions

3. Experimental Setup and Material Parameters in Ogden Model of Coronary Artery

3.1. Specimens for Tensile Tests

Porcine coronary arterial specimens were measured in this work. To maintain the artery mechanical properties from the live body to testing, all specimens were placed in phosphate buffered saline prior to testing. All tests were completed within 18 hours of slaughter [24]. The coronary artery specimens were from the anterior descending and circumflex coronary arteries. There were seven coronary specimens used for the arterial circumferential stretch (CS) test. The artery was placed between two thin slides as shown in Figure 1 to measure the specimen dimensions. The total thickness values (T), slide thicknesses (t_{g1} and t_{g2}), length L_o and width W_o were measured. The arterial wall thickness t_o was obtained by deducting t_{g1} and t_{g2} from T , as

$$t_o = \frac{T - (t_{g1} + t_{g2})}{2} \quad (8)$$

The coronary specimen shape was tubular. The specimen volume (V_o) was calculated from the measured length L_o , width W_o and arterial wall thickness t_o , as

$$V_o = L_o t_o [2(W_o - 2t_o) + \pi t_o]$$

$$\text{or } = \frac{L_o \pi [D_o^2 - (D_o - 2t_o)^2]}{4} \quad (9)$$

The outside diameter D_o of tubular specimen was estimated using Eq. (9) leading to

$$D_o = \frac{2}{\pi} [W_o + t_o(\pi - 2)] \quad (10)$$

The measured data for all specimens in the corresponding CS tests are listed in Table 1.

The tensile tests were measured using a 500N

SHIMADZU EZ-Test with the maximum stroke of 500 mm and measurement accuracy 0.01 mm. In the CS test the specimen was extended using two hooks as shown in Figure 2. The coronary arterial specimens were stretched and measured during the tensile test. A preload of 0.02 N was applied in these tests for the zero adjustment. The variation in tensile load and stroke were recorded continuously during the test. A high resolution digital camera was used to record the dimension variation. The correspondent stretch and stress variations were computed via the measured data. The loading speed in the CS test for coronary arteries was controlled at 4 mm/min.

3.2. Circumferential Stress-Stretch Curves in Arterial Circumferential Stretch (CS) Tests

During the arterial CS test, the specimen was stretched into an oval form as shown in Figure 3. The length L and the distance between hooks G were measured. To obtain the circumferential stress, the variation in sectional area of the specimen must be calculated during the test. Because the specimens were not deformed uniformly, an average sectional area was used in this work. Based on biological soft tissue being incompressible [7] assumption the specimen volume can be considered to be constant during loading. The variation in average cross section area of the measured specimen was estimated from the original volume and the measured specimen length L and distance between hooks G as shown in Figure 3. From the specimen shape, the average thickness t of the specimen during the test was derived using the following equation.

$$t = \frac{I}{\pi} \left[\sqrt{\left(G + d + \frac{\pi d}{2}\right)^2 + \frac{\pi V_o}{L}} - \left(G + d + \frac{\pi d}{2}\right) \right] \quad (11)$$

where V_o : is the volume of specimen.

L : is the measured length of specimen during the tensile test.

d : is the hook diameter.

G : is the measured distance between hooks during the tensile test.

t : is the average thickness of arterial specimen during the tensile test.

The variation in sectional area A and the average circumferential true stress σ_c of the measured arterial specimen was computed as

$$\sigma_c = \frac{F_c}{A} = \frac{F_c}{2tL}, \quad (12)$$

where F_c is the measured tensile load during the tensile test.

The corresponding circumferential stretch ratio value λ_c of the measured specimen was derived as

$$\lambda_c = \frac{C}{C_i} \tag{13}$$

With

$$C = 2(G+d) + \pi(d+t), \tag{14}$$

where c : is the circumferential stretch of specimen during the tensile test.

C : is the mean circumference of specimen during the tensile test.

C_i : is the initial mean circumference of specimen with preload applied only.

4. Measured Results and Curve Fitted Ogden Model Parameters

A number of coronary artery specimens were measured in the CS tests. The measured load-elongation curves in the corresponding artery CS tests are plotted in Figure 4. The different sizes of the specimens resulted in different load-elongation curves. The corresponding variation in true stress and stretch curves are shown in Figure 5. The applied strain rates ranged from 0.013% to 0.023% per-second as listed in Table 1. The variation in measured data and the corresponding true stress of specimen C1 was tabulated and illustrated in Table 2.

The elastic modulus of a coronary artery can be approximated as the tangential slope of the measured stress-stretch curve. The measured stress-stretch curves indicate that the elastic modulus is sensitive to the load. Roughly, the modulus variation can be divided into four stages as shown in Figure 6. In the first stage, the elastic modulus value is low. When the stress curve rises over the heel over point (HOP) [11], the loaded coronary artery goes into the transitional portion, i.e. the second stage. Figure 5 presents the HOP of a coronary artery circumferential curve located in the stretch range between 1.1 and 1.3. In the second stage a positive stress-stretch curve slope is observed. In other words, the modulus increases gradually with the load in this stage. An almost constant modulus remains in the following third stage. Generally, an abrupt modulus drop is observed after passing the peak load. An undulating stress-stretch curve is presented in the final fourth stage. However, the measured stress-stretch curves of some specimens, i.e. specimen C2 and C3, have only stages 1, 2 and 3 as shown in Figure 5. Most coronary arteries have a stress reduction when the stretch reaches around 1.4. In arterial histology, the main arterial wall composition elements are elastin, collagen and smooth muscle [25]. Collagen strength is much greater than that of elastin and smooth muscle. Therefore, some softer tissues failed during the test and the remaining tougher tissues continued to bear the load. This may be the reason for the stress undulation in the fourth stage as shown in Figures 5

and 6.

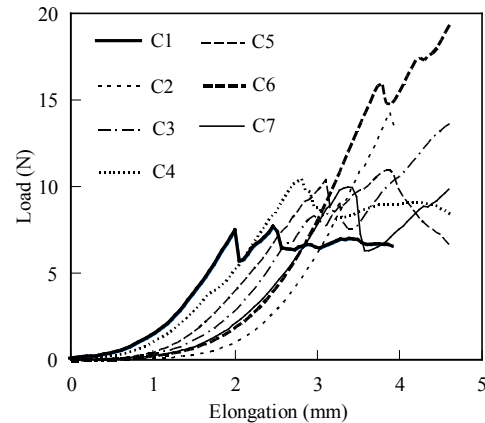


Figure 4. The variation in measured load-elongation curves for coronary artery specimens

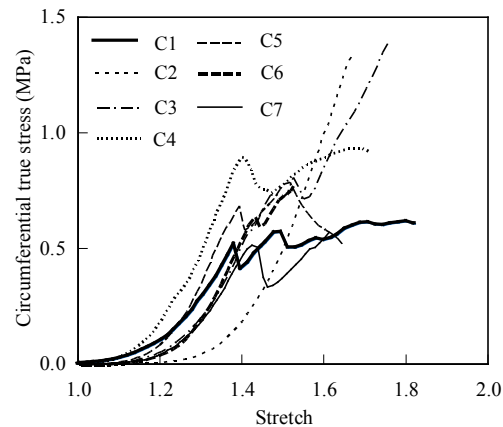


Figure 5. The variation in measured stress-stretch curves for coronary artery specimens

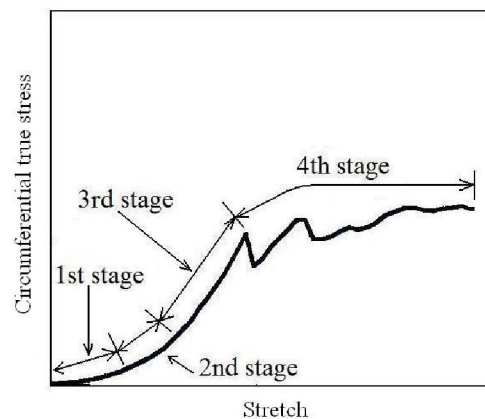
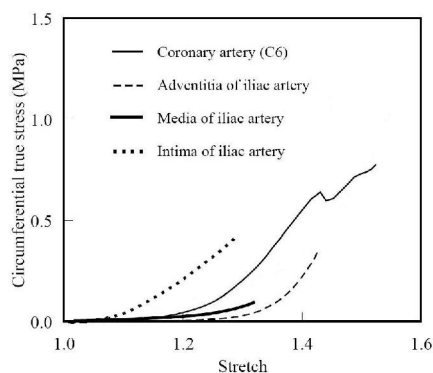


Figure 6. The four stages of modulus variation in measured stress-stretch curve

Table 2. Measured results for the coronary artery specimen C1 in the circumferential stretch test

| measured data | | | calculated values | | | | |
|-------------------|--|-------------------|------------------------------------|--------------------------------------|--|---|-------------------------------------|
| length (L) | distance between two hooks (G) | load (f_c) | arterial wall thickness (t) | axial sectional area (A_A) | specimen's girth at half thickness (C) | circumferential true stress (σ_c) | cir. stretch (ϵ_c) |
| (mm) | (mm) | (N) | (mm) | (mm^2) | (mm) | (N/mm^2) | (ϵ_c) |
| 10.99 | 0.13 | 0.000 | 0.89 | 19.36 | 8.17 | 0.00 | 1.00 |
| 10.99 | 0.14 | 0.025 | 0.88 | 19.25 | 8.19 | 0.00 | 1.00 |
| 10.99 | 0.17 | 0.054 | 0.87 | 19.14 | 8.22 | 0.00 | 1.01 |
| 10.97 | 0.28 | 0.119 | 0.86 | 18.77 | 8.38 | 0.01 | 1.03 |
| 10.93 | 0.52 | 0.268 | 0.82 | 17.95 | 8.76 | 0.01 | 1.07 |
| 10.92 | 0.69 | 0.454 | 0.80 | 17.44 | 9.02 | 0.03 | 1.10 |
| 10.90 | 0.78 | 0.592 | 0.79 | 17.15 | 9.17 | 0.03 | 1.12 |
| 10.89 | 0.96 | 1.000 | 0.76 | 16.63 | 9.46 | 0.06 | 1.16 |
| 10.87 | 1.11 | 1.391 | 0.75 | 16.21 | 9.70 | 0.09 | 1.19 |
| 10.84 | 1.28 | 1.963 | 0.73 | 15.77 | 9.98 | 0.12 | 1.22 |
| 10.76 | 1.41 | 2.638 | 0.72 | 15.41 | 10.21 | 0.17 | 1.25 |
| 10.70 | 1.56 | 3.534 | 0.70 | 15.03 | 10.47 | 0.24 | 1.28 |
| 10.70 | 1.69 | 4.413 | 0.69 | 14.73 | 10.68 | 0.30 | 1.31 |
| 10.70 | 1.84 | 5.435 | 0.67 | 14.39 | 10.93 | 0.38 | 1.34 |
| 10.65 | 2.05 | 7.208 | 0.65 | 13.93 | 11.30 | 0.52 | 1.38 |
| 10.65 | 2.22 | 5.943 | 0.64 | 13.59 | 11.57 | 0.44 | 1.42 |
| 10.65 | 2.37 | 6.735 | 0.62 | 13.29 | 11.83 | 0.51 | 1.45 |
| 10.57 | 2.51 | 7.378 | 0.62 | 13.02 | 12.09 | 0.57 | 1.48 |
| 10.55 | 2.67 | 6.382 | 0.60 | 12.72 | 12.37 | 0.50 | 1.51 |
| 10.55 | 2.83 | 6.367 | 0.59 | 12.44 | 12.64 | 0.51 | 1.55 |
| 10.51 | 2.99 | 6.585 | 0.58 | 12.17 | 12.93 | 0.54 | 1.58 |
| 10.44 | 3.15 | 6.482 | 0.57 | 11.89 | 13.23 | 0.55 | 1.62 |
| 10.37 | 3.30 | 6.788 | 0.56 | 11.65 | 13.51 | 0.58 | 1.65 |
| 10.29 | 3.46 | 6.935 | 0.55 | 11.40 | 13.80 | 0.61 | 1.69 |
| 10.19 | 3.63 | 6.704 | 0.55 | 11.15 | 14.11 | 0.60 | 1.73 |
| 10.11 | 3.78 | 6.624 | 0.54 | 10.92 | 14.40 | 0.61 | 1.76 |
| 10.05 | 3.87 | 6.607 | 0.54 | 10.80 | 14.57 | 0.61 | 1.78 |
| 9.99 | 3.95 | 6.576 | 0.53 | 10.69 | 14.72 | 0.62 | 1.80 |
| 9.91 | 4.04 | 6.399 | 0.53 | 10.56 | 14.90 | 0.61 | 1.82 |

**Figure 7.** The measured stress-stretch data from specimen C6 and the published data

In anatomy, the artery includes three main layers i.e. adventitia, media and intima [25]. The measured stress-stretch curve of specimen C6 was compared with the published stress-stretch curves for an iliac artery [7], as shown in Figure 7. The results in Figure 7 indicate that the data measured from the proposed CS test agrees with the published data [7]. Within the stress range from 0.2 to 0.4 MPa, the adventitia and intima moduli vary within 2.0 and 4.8 MPa. This agrees with the aforementioned modulus range for coronary arteries.

For simplicity, the coronary artery is considered to be extended in the circumferential direction. The axial deformation effect is so small that it can be ignored. Therefore, the nonlinear strain energy

function, i.e. Equation (7), was introduced to derive the stress-stretch relationships of coronary artery and plaque in simulation. Based on the coronary artery incompressibility assumption, i.e. $J = \lambda_1 \lambda_2 \lambda_3 = 1$, three principal stretches can be approximated as $\lambda_2 = \lambda_3 = \lambda_1^{-1/2}$ in uniaxial tensile condition. The corresponding uniaxial true stress can then be expressed in terms of uniaxial stretch as

$$\sigma_I = \sum_{n=1}^N \mu_n \left(\lambda_I^{\alpha_n} - \lambda_I^{-\frac{\alpha_n}{2}} \right) \quad (15)$$

For getting a good curve fitting and also considering computational efficiency, the item number $N=2$ was used in this study. It leads to

$$\sigma_I = \mu_1 \left(\lambda_I^{\alpha_1} - \lambda_I^{-\frac{\alpha_1}{2}} \right) + \mu_2 \left(\lambda_I^{\alpha_2} - \lambda_I^{-\frac{\alpha_2}{2}} \right) \quad (16)$$

Table 3. Curve fitted Ogden model parameters for coronary artery and plaque

| | (MPa) | (MPa) | | |
|----------|------------------------|------------------------|-------|------------------------|
| artery* | 1.755×10^{-2} | -11.39 | 10.79 | 1.661×10^{-2} |
| plaque** | 1.437×10^{-3} | 4.366×10^{-9} | 45.03 | 32.48 |

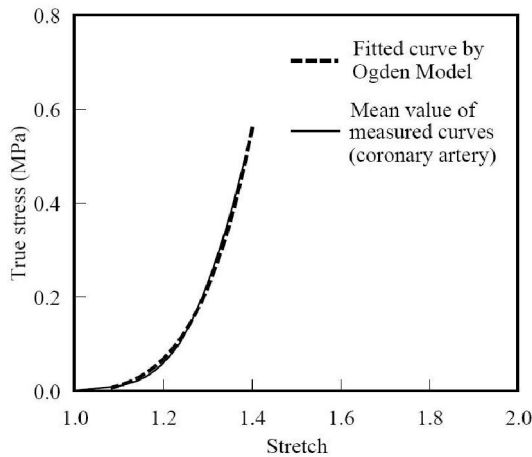
*: The Ogden model parameters fitted from the measured data proposed in this study.

** : The Ogden model parameters fitted from the published data [7].

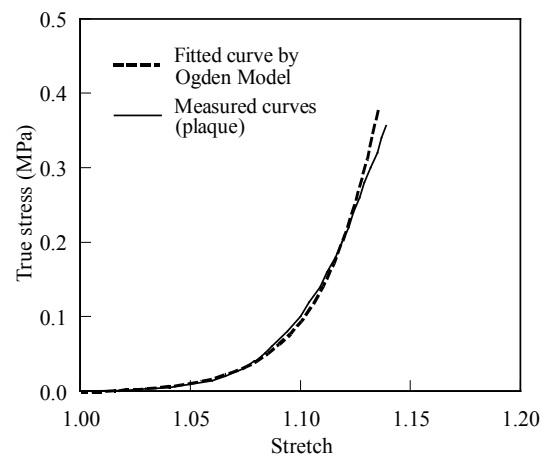
The least-squares method was applied to curve fitted all the material parameters, and from the measured coronary artery circumferential stress-stretch curves. The mean stretch value of

different curves, corresponding to same true stress, was computed first. The stress from 0 to 5.0 N/mm², 20 equally-spaced points were chosen for computing the mean value of measured curves as shown in Figure 8(a). The same method was applied to curve fit the measured plaque data which cited from the literature [7]. The extracted material constants are listed in Table 3. The difference between the measured and fitted plaque curves is shown in Figure 8(b).

The feasibility of the proposed Ogden mechanical coronary artery model is illustrated in this work using a stent implantation process simulated using the elastic-plastic finite element method. The traditional Palmaz type stent, the initially folded balloon and discontinuous distributed plaque were included in the simulation model. Figure 9 shows the 1/16 symmetrical three-dimensional model with a 1/8 circumferential and 1/2 axial symmetry component. The corresponding dimensions and material properties of the different parts in the finite element model are listed in Table 4. The simulated stent implantation under different pressures is shown in Figure 10. The stent diameter variation in the inflation and deflation process can be simulated using the proposed coronary artery material properties. The artery also causes an elastic recoil in the stent diameter during the deflation process. The simulated results indicate that the proposed Ogden coronary artery mechanical model is adequate to simulate the stent implantation process.



(a) Coronary artery



(b) Plaque

Figure 8. Ogden model fitted stress-stretch curves for coronary artery and plaque

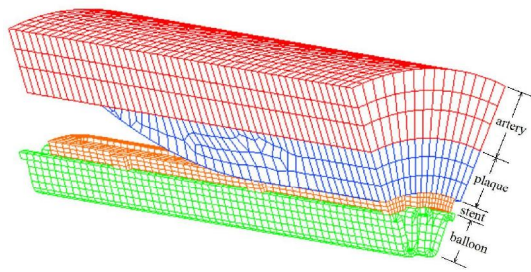


Figure 9. The 1/8 circumferential and 1/2 axial symmetry finite element model for stent implantation simulation

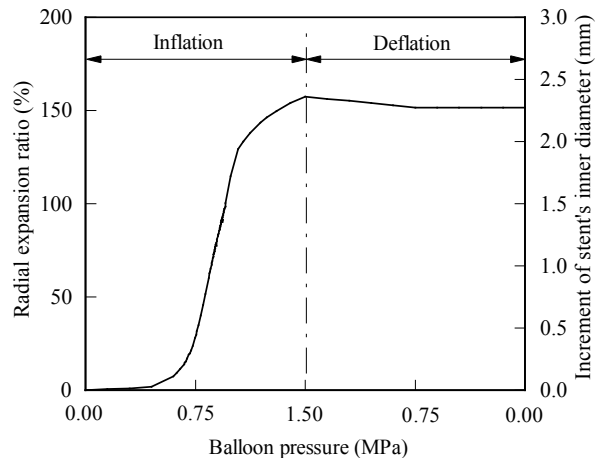


Figure 10. The simulated stent implantation under different pressures

Table 4. Component dimensions and material properties in the illustrated example

| item | arterial wall | plaque | stent | balloon |
|-----------------------|----------------------|----------------------|---------------|----------------|
| outer diameter (mm) | 3.5 | 2.5 | 1.7 | nil |
| thickness (mm) | 0.5 | 0.4 | 0.1 | 0.05 |
| length (mm) | 4.284 | 3.360 | 4.284 | 4.284 |
| material model | nonlinear (Ogden) | nonlinear (Ogden) | elastoplastic | linear elastic |
| Young's modulus (GPa) | nil | nil | 196 | 0.69 |
| Poisson's ratio | nil | nil | 0.3 | 0.3 |

5. Conclusions

This article proposed a nonlinear Ogden material model for the stent implantation process in a deformed coronary artery. The corresponding Ogden model parameters were derived by collecting the stress-stretch values from over seven coronary artery specimens. The data may be able to provide valuable samples for deriving the stress-stretch function of the coronary specimen when the applied load is not over the heel over point (HOP).

For validation, the proposed nonlinear Ogden material model for coronary artery was applied to a Palmaz type stent implantation process. The simulated stent deformation was found to be reasonable. It had a good correlation with the measured results. However, since the material parameters were derived only from coronary artery specimens, the use of the material parameters for different types of arteries should be done with caution.

Acknowledgments

This research was supported by the National Science Council through grant NSC97-2221-E-110-022 -MY3. The authors gratefully acknowledge Dr. Y. C. Wang (Div. of

Cardiology, Dept. of Internal Medicine, Kaohsiung Armed Forces General Hospital, Kaohsiung, Taiwan) for their kind help with specimens' preparation and data collection.

*Correspondence:

Jaoh-Hwa Kuang

E-mail: kuang@faculty.nsysu.edu.tw

References

1. C. Feezor, A. Tajaddini, D. Kilpatrick, D.G. Vince, D. Jacobson, Integration of animal and human coronary tissue testing with finite element techniques for assessing differences in arterial behavior, American Society of Mechanical Engineers, Bioengineering Division, 2001, 50:135-136.
2. C.J. van Andel, P.V. Pistecky, C. Borst, Mechanical properties of coronary arteries and internal mammary arteries beyond physiological deformations, In proceedings of the 23th Annual EMBS International Conference, Istanbul, Turkey, 2001:113-115.
3. C.J. van Andel, P.V. Pistecky, C. Borst, Mechanical properties of porcine and human arteries: implications for coronary anastomotic connectors, The Annals of Thoracic Surgery, 2003, 76:58-64.

4. M. Carboni, G.W. Desch, H.W. Weizsacker, Passive mechanical properties of porcine left circumflex artery and its mathematical description, *Medical Engineering & Physics*, 2007, 29:8-16.
5. A. Pandit, X. Lu, C. Wang, G.S. Kassab, Biaxial elastic material properties of porcine coronary media and adventitia, *American Journal of Physiology-Heart and Circulatory Physiology*, 2005, 288:2581-2587.
6. C. Wang, M. Garcia, X. Lu, Y. Lanir, G.S. Kassab, Three-dimensional mechanical properties of porcine coronary arteries: a validated two-layer model, *American Journal of Physiology-Heart and Circulatory Physiology*, 2006, 291:1200-1209.
7. G.A. Holzapfel, C.A.J. Schulze-Bauer, M. Stadler, Mechanics of angioplasty: wall, balloon and stent, *American Society of Mechanical Engineers, Applied Mechanics Division*, 2000, 242:141-154.
8. K.L. Monson, W. Goldsmith, Axial mechanical properties of fresh human cerebral blood vessels, *Journal of Biomechanical Engineering*, 2003, 125:288-294.
9. K.L. Monson, W. Goldsmith, N.M. Barbaro, G.T. Manley, Significance of source and size in the mechanical response of human cerebral blood vessels, *Journal of Biomechanics*, 2005, 38:737-744.
10. F.H. Silver, P.B. Snowhill, D.J. Foran, Mechanical behavior of vessel wall: a comparative study of aorta, vena cava, and carotid artery, *Annals of Biomedical Engineering*, 2003, 31:793-803.
11. P.B. Snowhill, F.H. Silver, A mechanical model of porcine vascular tissues-Part II: stress-strain and mechanical properties of juvenile porcine blood vessels, *Cardiovascular Engineering: An International Journal*, 2005, 5:157-169.
12. N. Gundiah, M.B. Ratcliffe, L.A. Pruitt, Determination of strain energy function for arterial elastin: Experiments using histology and mechanical tests, *Journal of Biomechanics*, 2007, 40:586-594.
13. M.A. Lillie, J.M. Gosline, Mechanical properties of elastin along the thoracic aorta in the pig, *Journal of Biomechanics*, 2007, 40:2214-2221.
14. C. Lally, A.J. Reid, P.J. Prendergast, Elastic behavior of porcine coronary artery tissue under uniaxial and equibiaxial tension, *Annals of Biomedical Engineering*, 2004, 32:1355-1364.
15. C. Lally, F. Dlan, P.J. Prendergast, Cardiovascular stent design and vessel stresses: a finite element analysis, *Journal of Biomechanics*, 2005, 38:1574-1581.
16. L. Gu, S. Santra, R.A. Mericle, A.V. Kumar, Finite element analysis of covered microstents, *Journal of Biomechanics*, 2005, 38:1221-1227.
17. L. Machan, Clinical experience and applications of drug-eluting stents in the noncoronary vasculature, bile duct and esophagus, *Advanced Drug Delivery Reviews*, 2006, 58:447-462.
18. K. Takahata, Y.B. Gianchandani, A planar approach for manufacturing cardiac stents: design, fabrication, and mechanical evaluation, *Journal of Microelectromechanical Systems*, 2004, 13:933-939.
19. W. Wu, M. Qi, X.P. Liu, D.Z. Yang, W.Q. Wang, Delivery and release of nitinol stent in carotid artery and their interactions: A Finite element analysis, *Journal of Biomechanics*, 2007, 40:3034-3040.
20. S.K. Lam, G.S.K. Fung, S.W.K. Cheng, K.W. Chow, A computational investigation on the effect of biomechanical factors related to stent-graft models in the thoracic aorta, In proceedings of the 29th Annual International Conference of the IEEE Engineering in Medicine and Biology Society, Lyon, France, 2007:943-946.
21. Z. Li, C. Kleinstreuer, Computational analysis of type II endoleaks in a stented abdominal aortic aneurysm model, *Journal of Biomechanics*, 2006, 39:2573-2582.
22. S. Miyamoto, T. Hadama, H. Anai, H. Sako, O. Shigemitsu, E. Iwata, H. Hmamamoto, Successful open stent grafting of a right aortic arch and a descending aortic aneurysm originating from a kommerell's diverticulum: report of a case, *Surgery Today*, 2002, 32:359-361.
23. G.A. Holzapfel, *Nonlinear Solid Mechanics*, John Wiley & Sons, West Sussex, England, 2000:205-225.
24. A.O. Medynsky, D.W. Holdsworth, M.H. Sherbrin, R.N. Rankin, M.R. Roach, The effect of storage time and repeated measurements on the elastic properties of isolated porcine aortas using high resolution x-ray CT, *Canadian Journal of Physiology and Pharmacology*, 1998, 76:451-456.
25. K. Hayashi, J.D. Humphrey, R.W. Ogden, G.A. Holzapfel, A.D. McCulloch, A. Rachev, T.P. Usyk, Biomechanics of soft tissue in cardiovascular systems. In: Holzapfel GA, Ogden RW (Eds.), *Courses and lectures- No.441 of international center for mechanical sciences in Udine, Italy 2001*, Springer Wein, New York, USA, 2003:16-29.

11/1/2011